AFRL-AFOSR-VA-TR-2022-0040

Predictive Model-Assisted Guided Wave Structural Health Monitoring

Furse, Cynthia
UNIVERSITY OF UTAH SALT LAKE CITY
201 PRESIDENTS CIR RM 408
SALT LAKE CITY, UT,
US

09/27/2021
Final Technical Report

Air Force Research Laboratory
Air Force Office of Scientific Research
Arlington, Virginia 22203
Air Force Materiel Command

REPORT DOCUMENTATION PAGE

Form Approved
OMB No. 0704-0188

1. REPORT DATE *(DD-MM-YYYY)*	**2. REPORT TYPE**	**3. DATES COVERED** *(From - To)*
27-09-2021	Final	01 Mar 2017 - 28 Feb 2021

4. TITLE AND SUBTITLE
Predictive Model-Assisted Guided Wave Structural Health Monitoring

5a. CONTRACT NUMBER

5b. GRANT NUMBER
FA9550-17-1-0126

5c. PROGRAM ELEMENT NUMBER
61102F

6. AUTHOR(S)
Cynthia Furse

5d. PROJECT NUMBER

5e. TASK NUMBER

5f. WORK UNIT NUMBER

7. PERFORMING ORGANIZATION NAME(S) AND ADDRESS(ES)
UNIVERSITY OF UTAH SALT LAKE CITY
201 PRESIDENTS CIR RM 408
SALT LAKE CITY, UT
US

8. PERFORMING ORGANIZATION REPORT NUMBER

9. SPONSORING/MONITORING AGENCY NAME(S) AND ADDRESS(ES)
AF Office of Scientific Research
875 N. Randolph St. Room 3112
Arlington, VA 22203

10. SPONSOR/MONITOR'S ACRONYM(S)
AFRL/AFOSR RTA1

11. SPONSOR/MONITOR'S REPORT NUMBER(S)
AFRL-AFOSR-VA-TR-2022-0040

12. DISTRIBUTION/AVAILABILITY STATEMENT
A Distribution Unlimited: PB Public Release

13. SUPPLEMENTARY NOTES

14. ABSTRACT
Our research objective is to enable guided wave monitoring for inaccessible, complex geometric structures. These systems have a significant potential to improve the sustainability and survivability of United States Air Force aircraft and munitions. However, current guided wave structural health monitoring systems are designed for simple geometric structures, such as large, rectangular plates. Aircraft and other structures are more geometrically complex and contain common structural elements, including fasteners and stiffeners that complicate wavefields. Complexity is one of the Air Force's foundational challenges for creating enhanced damage detection systems. Numerical simulations have helped us to understand wave propagation in complex structures. Yet, these simulations rarely match experimental data. As a result, these simulations cannot significantly improve data analysis. We address this technical gap by integrating large numerical guided wave models with experimental data to predict wave propagation and to exploit geometric complexities for damage localization and characterization. Our approach is fundamentally different from previous work because our algorithms require no explicit parameterizations (e.g., Young's modulus, temperature, etc.) that restrict models to very specific solutions. We instead exploit the sparse, modal representations of waves that implicitly describe parameters. Funds have been used to support students that conduct this research and the principal investigator that directs this research.

15. SUBJECT TERMS

16. SECURITY CLASSIFICATION OF:			**17. LIMITATION OF ABSTRACT**	**18. NUMBER OF PAGES**	**19a. NAME OF RESPONSIBLE PERSON**
a. REPORT	**b. ABSTRACT**	**c. THIS PAGE**			MARTIN SCHMIDT
U	U	U	UU	21	**19b. TELEPHONE NUMBER** *(Include area code)* 588-8436

AFOSR Final Performance Report

Award Title: (YIP) Predictive, Model-Assisted Guided Wave Structural Health Monitoring
Award: FA9550-17-1-0126
Written by: Joel B. Harley

Project Abstract

Our research objective is to enable guided wave monitoring for inaccessible, complex geometric structures. These systems have a significant potential to improve the sustainability and survivability of United States Air Force aircraft and munitions. However, current guided wave structural health monitoring systems are designed for simple geometric structures, such as large, rectangular plates. Aircraft and other structures are more geometrically complex and contain common structural elements, including fasteners and stiffeners that complicate wavefields. Complexity is one of the Air Force's foundational challenges for creating enhanced damage detection systems.

Numerical simulations have helped us to understand wave propagation in complex structures. Yet, these simulations rarely match experimental data. As a result, these simulations cannot significantly improve data analysis. We address this technical gap by integrating large numerical guided wave models with experimental data to predict wave propagation and to exploit geometric complexities for damage localization and characterization. Our approach is fundamentally different from previous work because our algorithms require no explicit parameterizations (e.g., Young's modulus, temperature, etc.) that restrict models to very specific solutions. We instead exploit the sparse, modal representations of waves that implicitly describe parameters.

Funds have been used to support students that conduct this research and the principal investigator that directs this research.

Supported Researchers

- Cynthia Furse, Professor, University of Utah
  - Administrative PI
- Joel B. Harley, Assistant Professor, University of Florida
  - Technical Lead / Original PI
- K. Supreet Alguri, PhD Student, University of Utah
- Soroosh Sabeti, PhD Student, University of Utah
- Ishan Khurjekar, PhD Student, University of Florida
- Harsha Tetali, PhD Student, University of Florida

Collaborating Researchers

- Joseph Melville, MS Student, University of Utah
- Alexander C.S. Douglass, Ph.D. Student, University of Utah / Air Force Research Lab
- Daniel Sparkman, Researcher, Air Force Research Lab
- Chen Ciang Chia, Senior Lecturer, Universiti Putra Malaysia (shared data)
- Cara A.C. Leckey, NASA Langley (shared data)

- Luca De Marchi, University of Bologna (shared data)
- Christopher Deemer, Engineer, Orbital ATK

Cumulative Research Products

Journal Papers

(1) I.D. Khurjekar and J.B. Harley, "Sim-to-Real Localization: Environment Resilient Deep Learning Models for Guided Wave based Damage Localization," in preparation.

(2) H.V. Tetali and J.B. Harley, "Unsupervised Learning of Wave Representations with Physics-Informed Dictionary Learning," in preparation.

(3) K.S. Alguri, C.C. Chia, and J.B. Harley, "Sim-to-Real: Employing ultrasonic guided wave digital surrogates and transfer learning for damage visualization," Ultrasonics, vol. 111, p. 106338, Mar. 2021.

(4) S. Sabeti and J. B. Harley, "Spatio-temporal undersampling: Recovering ultrasonic guided wavefields from incomplete data with compressive sensing," Mech. Syst. Signal Process., vol. 140, p. 106694, Jun. 2020.

(5) A.C.S. Douglass, D. Sparkman, and J. B. Harley, "Segmentation of Hidden Delaminations with Pitch–Catch Ultrasonic Testing and Agglomerative Clustering," J. Nondestr. Eval., vol. 39, no. 1, p. 8, Jan. 2020.

(6) S. Sabeti, C.A.C. Leckey, L. De Marchi, J.B. Harley, "Sparse Wavenumber Recovery and Prediction of Anisotropic Guided Waves in Composites," IEEE Ultrasonics, Ferroelectrics, and Frequency Control, vol. 66, no. 8, Aug. 2019.

(7) K.S. Alguri, J.B. Harley, "Baseline-Free Guided Wave Damage Detection with Surrogate Data and Dictionary Learning," Journal of the Acoustical Society of America, vol. 143, no.6, p. 3807, Jun. 2018.

Conference Proceedings

(1) J. B. Harley, K. S. Alguri, H. V. Tetali, S. Sabeti, "Learning Guided Wave Dispersion Curves from Multi-Path Reflections with Compressive Sensing," Proc. of the International Workshop on Structural Health Monitoring, pp. 1-9, 2019.

(2) H. V. Tetali, K. Supreet Alguri, and J. B. Harley, "Beyond black-box dictionary learning for waves." Proc. of the Machine Learning and the Physical Sciences Workshop at the Conference on Neural Information Processing Systems (NeurIPS), pp. 1-5, 2019.

(3) H. V. Tetali, K. S. Alguri, and J. B. Harley, "Wave Physics Informed Dictionary Learning In One Dimension," in 2019 IEEE 29th International Workshop on Machine Learning for Signal Processing (MLSP), 2019, pp. 1–6.

(4) I. Khurjekar and J. Harley, "Deep neural network-based guided wave damage localization," Review of Progress in Quantitative Nondestructive Evaluation, no. 0, Dec. 2019.

(5) S. Sabeti and J. B. Harley, "Polar sparse wavenumber analysis for guided wave reconstruction," in Proc. of the Review of Quantitative Nondestructive Evaluation, 2019, vol. 2102, p. 050012.

(6) H. V. Tetali, K. S. Alguri, and J. B. Harley, "Wave Physics Informed Dictionary Learning In One Dimension," in 2019 IEEE 29th International Workshop on Machine Learning for Signal Processing (MLSP), 2019, pp. 1–6.

(7) K. S. Alguri and J. B. Harley, "Transfer learning of ultrasonic guided waves using autoencoders: A preliminary study," in Proc. of the Review of Quantitative Nondestructive Evaluation, 2019, vol. 2102, p. 050013.

(8) K. S. Alguri, J. Melville, C. Deemer, and J. B. Harley, "Overcoming complexities: Damage detection using dictionary learning framework," in Proc. of the Review of Quantitative Nondestructive Evaluation, 2018, vol. 1949, p. 230006.

(9) J. Melville, K. S. Alguri, C. Deemer, and J. B. Harley, "Structural damage detection using deep learning of ultrasonic guided waves," in Proc. of the Review of Quantitative Nondestructive Evaluation, 2018, vol. 1949, p. 230004.

(10) S. Sabeti and J. B. Harley, "Two-dimensional sparse wavenumber recovery for guided wavefields," in Proc. of the Review of Quantitative Nondestructive Evaluation, 2018, vol. 1949, p. 230003.

(11) K. Supreet Alguri, Chen Ciang Chia, Joel B. Harley, "Model-driven, Wavefield Baseline Subtraction for Damage Visualization using Dictionary Learning," in Proc. of the International Workshop on Structural Health Monitoring, 2018.

(12) S. Sabeti and J. B. Harley, "Guided wave retrieval from temporally undersampled data," in 2017 IEEE International Ultrasonics Symposium (IUS), Washington, DC, 2017, pp. 1–4.

Archived Preprints

(1) I. D. Khurjekar and J. B. Harley, "Accounting for Physics Uncertainty in Ultrasonic Wave Propagation using Deep Learning," arXiv [cs.LG], 07-Nov-2019.

(2) I. D. Khurjekar and J. B. Harley, "Uncertainty Aware Deep Neural Network for Multistatic Localization with Application to Ultrasonic Structural Health Monitoring," arXiv [eess.SP], 14-Jul-2020.

Dissertations

(1) K. S. Alguri, "Transfer Learning of Ultrasonic Guided-Waves For Damage Isolation, Localization, and Detection," PhD, University of Utah, 2019.

(2) S. Sabeti, "Characterization and Prediction of Guided Wave Propagation in Complex Media via Compressive Sampling in Time and Space," PhD, University of Utah, 2019.

Synergistic Activities Enabled by this Funding

(1) 2018 & 2020, Summer Faculty Fellow at AFRL / RXCA

(2) 2018-2021, Co-Chair Review of Quantitative Nondestructive Evaluation session on Machine Learning and Statistical Methods in NDE with Daniel Sparkman from AFRL / RXCA

(3) 2019, Instructor of AFRL "Artificial Intelligence and Machine Learning Fundamentals Training Course"

Introduction

Guided wave structural health monitoring systems have the potential to significantly improve the sustainability and survivability of United States Air Force aircraft and munitions by monitoring inaccessible and critical components. In the last decade, fundamental tools for guided wave monitoring have been created. Yet, these tools are still limited to monitoring simple geometric structures, such as large, rectangular plates. For example, current guided wave technology cannot reliably monitor structures with stiffeners or stringers, which are integral to the structure of the airplane. To resolve this challenge, there has been recent research [1–3] into creating simulation tools to analyze guided waves in complex structures. Yet, there is a significant obstacle to using these simulations: *simulations rarely match experimental data.*

Simulations rarely match experimental data due to uncertainties: environmental variations [4], structural changes [5], degradation of sensors [6], and other factors that are unknown or unreasonable to model. A common approach to this challenge is to parameterize and model all of these factors to create many possible "alternative" models [7–9]. Yet, the computational requirements for tuning and constructing vast model libraries for each application are computationally and monetarily prohibitive. Ideally, we can instead use machine learning algorithms to extract these uncertainties from a combination of guided wave models and experimental data. If successfully, these hybrid simulation systems can predict data from simulation-like information with characteristics (i.e., these uncertainties) extracted from the experimental data.

Truly predictive nondestructive testing and structural health monitoring models will improve inspection accuracies, minimize inspection costs, improve safety, reduce the need for excessive data, and create pathways for new system-wide monitoring methods [1]. Predictive models will allow us to interrogate inaccessible, interconnected regions deep within a structure, such as a wing, that cannot easily be monitored or inspected. This will reduce costs associated with the need to disassemble many components for inspection through manual processes. Predictive models will also enable us to transition diagnostic information into prognostic information by enabling us to predict the future behavior of a tuned structural model from diagnostic data.

Hence, the objective of this project was to inestigate predictive models that fit numerical simulations with experimental data. Our predictive models are fundamentally different from previous modeling work [1, 3, 10, 11] because the original simulations act only as a guide for data analysis and we require no explicit parameterizations (e.g., Young's modulus, temperature, etc.) that restrict models to very specific solutions.. Our models integrate experimental data with either analytical (theoretically derived), numerical (obtained from numerical simulations), or experimental (measured from surrogate systems) models. We combine our models using sparse, modal information (i.e., a dictionary and its coefficient) that characterize how waves behave.

To achieve our objective, we created a collection of novel algorithms that combine simulated and experimental data under different circumstances. These algorithms are illustrated in Figure 1. The algorithms are divided into two categories a "Model-fitting Paradigm," where we have an underlying analytical wave propagation model, and a "Transfer Learning Paradigm," where that underlying model is learned from simulations or related experiments. The "Model-fitting Paradigm" utilizes a combination of wave physics knowledge with compressive sensing theory [12, 13] to learn the underlying representation of data. The "Transfer Learning Paradigm" uses dictionary learning [14] and sparse coding algorithms to learn an underlying model of the data. Throughout this project, we created these models and then demonstrated how they can be used for damage detection, localization, and characterization.

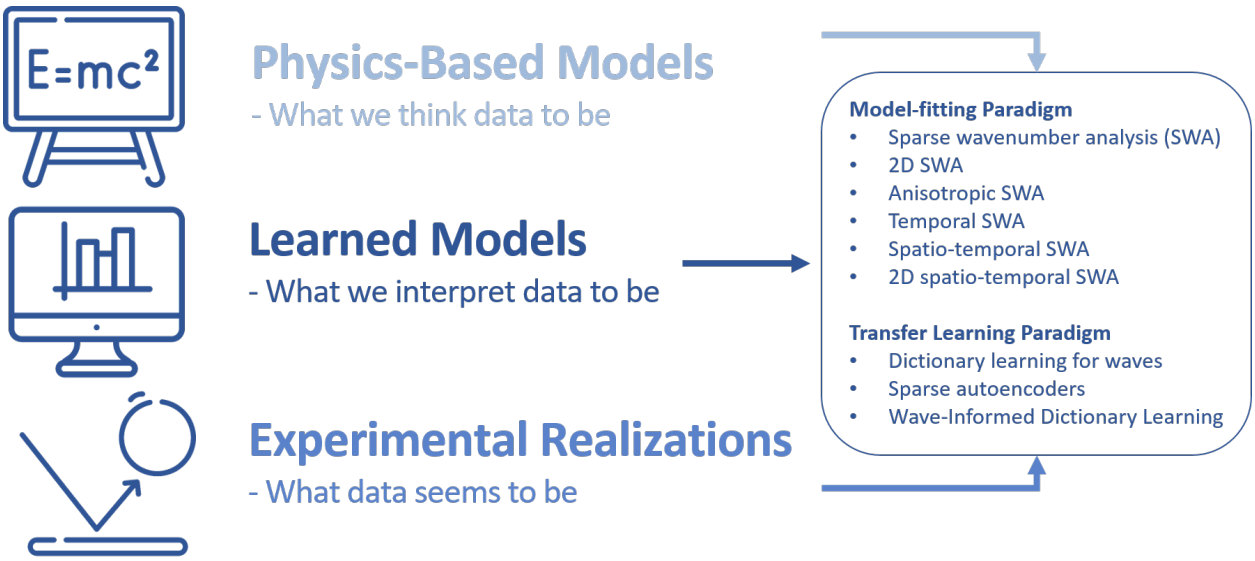

Figure 1: Illustration of our strategy and the algorithms created from this strategy.

Background: Challenges and Prior Art

Guided Waves

Guided waves, i.e., waves that are guided by the geometry of a structure or waveguide, are a widely researched tool for detecting, locating, and characterizing damage in physical structures [15–17]. Over the last two decades, *in situ* guided wave structural health monitoring research has established robust tools for the continuous inspection and monitoring of large structural areas. However, current guided wave structural health monitoring tools are mostly designed for simple geometric structures, such as large, rectangular plates. The multiple modes and multiple reflections of guided waves in complex geometric structures significantly reduce the effectiveness of current damage localization and characterization algorithms. As a result, guided wave technologies are not yet adequate for a large variety of complex, mechanical structures that would be invaluable to monitor. This project addressed this challenge with predictive models that merge numerical simulations of complex structures with experimental observations.

Guided waves can interrogate large areas with relatively low attenuation and are sensitive to most forms of damage. Guided waves have been implemented in a large variety of structural systems, including pipelines [16, 18–23], bridges [24, 25], concrete [26], steel cables [27–29], metal aircraft components [30, 31], and composite aircraft components [1, 32–34]. One of the most significant challenges for working with guided waves is the complexity of measured signals.

Guided wave damage detection, localization, and characterization methods can be classified as sparse array [35–38], dense array (i.e., beamforming) [39, 40], or wavefield methods. We focus on sparse arrays and wavefield methods. Sparse arrays can monitor large areas as they provide unique information about the wavefield at each sensor. The most popular sparse array localization methods include time-reversal [41–43], delay-and-sum [36, 44, 45], and delay-and-sum variants [38, 46]. Time reversal uses prior experimental wavefield measurements to achieve super-resolution performance in complex structures. However, obtaining experimental wavefields is often impractical and time-reversal can be very sensitive to environmental variations. Delay-and-sum methods assume the waves are

represented by a single dominant mode traveling at a single velocity. In these methods, the signal's envelopes (instead of the raw data) are often processed to reduce errors between the model (a delay) and measured data, although this results in high location uncertainty. The delay-and-sum variants aim to often reduce this uncertainty through the incorporation of known physics.

Wavefield methods capture a spatial region of propagation, usually with a laser Doppler vibrometer [32] or air-coupled ultrasonic transducer [47]. Methods such as local energy analysis [48] or local wavenumber analysis [49, 50] have been used to detect and locate damage with this data. While wavefield data is considerably more difficult to obtain than array data, it is a leading approach for detecting many types of hidden defects, such as delaminations [51], in composite materials.

Inadequacy of Simulations

Many similar platforms now exist for generating guided waves [52]. These platforms provide invaluable insights and guides for analyzing and processing data. However, these platforms are alone inadequate for the direct processing of experimental data. This is because seemingly small variations between experimental and simulated data cause large changes in the data processing.

As an example, we can consider subtraction. Baseline subtraction (subtracting data from a healthy specimen with data from a damaged specimen) is a common approach for isolating reflections from damage [6]. Collecting a useful baseline is a challenge due to the baseline needing to be collected early in the life of the system and all of the benign variations (which change the data) between then and the time the damage forms. Figure 2 visually illustrates how small changes in guided wave parameters can adversely affect processing capabilities. We illustrate a guided wave simulation with velocity v and Gaussian enveloped frequency response, the same guided wave simulation with a small variation in velocity (1%) as well as a scatterer in the center of the space, and the difference between these two simulations. Ideally, the difference would isolate the reflections from the scatterer. However, the small variations keep the reflections mostly hidden. This illustrates the need to adapt the simulations to better match our the uncertainties within the data.

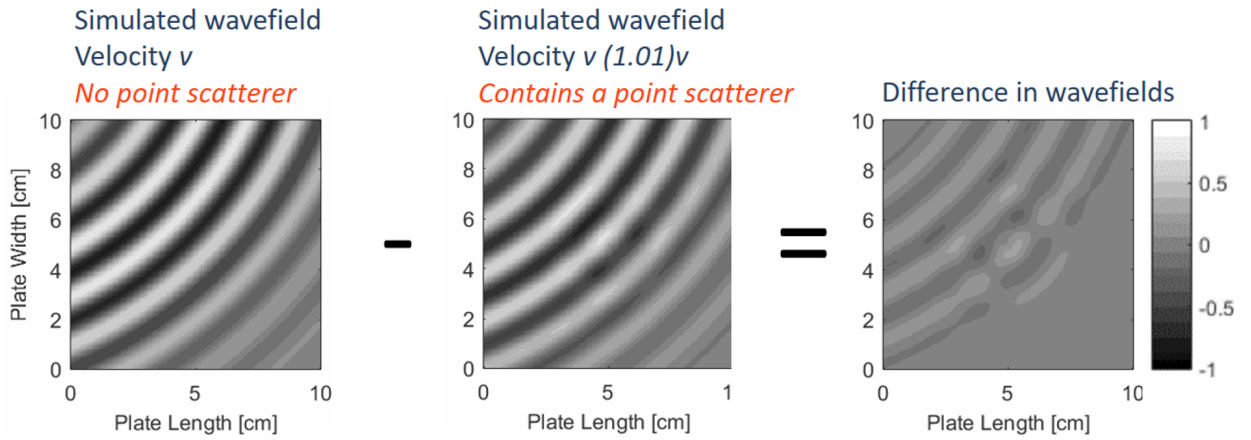

Figure 2: Illustration of how small changes in guided wave parameters can adversely affect processing capabilities. From left to right, we illustrate a guided wave simulation with velocity v, the same guided wave simulation with a 1% variation in velocity as well as a scatterer in the center of the space, and the difference between these simulations.

Sparse Representations: The Model-fitting Paradigm

Our framework is based on the fact that waves, at each frequency, can be represented by a linear (often sparse) combination of modes [53, 54]. By discretizing the frequencies and modes, this statement can be mathematically expressed as

$$\mathbf{X} = \mathbf{\Phi}\mathbf{V} \tag{1}$$

where $\mathbf{X}$ is an $M \times Q$ (measurements by frequencies) data matrix, $\mathbf{\Phi}$ is an $M \times N$ (measurements by user-determined elements) basis matrix or dictionary of modes, and $\mathbf{V}$ is a sparse $N \times Q$ (user-determined elements by frequencies) matrix that defines what modes are at each frequency. So, for example, in a one-dimensional string, each mode (i.e., a column of $\mathbf{\Phi}$) corresponds to a wavenumber. For a standing wave, only harmonic wavenumbers exist. For a traveling wave, an infinite number of wavenumbers / modes may exist. Yet, at *any given frequency*, the traveling wave only ever has one wavenumber / mode present. For more complex waves, such as guided waves, additional modes are often present at each frequency. These modes may have complex spatial shapes depending on the structure of interest.

In our "Model-fitting Paradigm," we determine $\mathbf{\Phi}$ from theory and assume $\mathbf{V}$ to be sparse. Since $\mathbf{V}$ is sparse, we can use compressive sensing and sparse coding methods [12, 55, 56] to solve this problem. Sparse representations have been used in a wide variety of applications, including compressive sensing [12, 55], single-pixel cameras [57], image [58] and video [59] processing, magnetic resonance imaging [60], and seismology [61]. Once $\mathbf{V}$ is learned, $\mathbf{\Phi}$ can be changed based on the known analytical formula for wave propagation. The two matrices are then multiplied to predict new wave behavior.

Dictionary Learning

In our "Transfer Learning Paradigm," we use dictionary learning to extract possible full wavefield modes from numerical simulations. Mathematically, this means we extract both $\mathbf{D}$ and $\mathbf{V}$ from data. We usually learn from some form of surrogate data, which may be simulation or experimental. The matrix $\mathbf{D}$ represents the "modes" of the waves. The term $\mathbf{V}$ represents the linear combination coefficients of those modes in the data. We learn $\mathbf{D}$ (and a structure-specific $\mathbf{V}$) from our surrogate data (such as a simulation). Then given $\mathbf{D}$, we can learn a new $\mathbf{V}$ that is tuned specifically to a different experimental dataset.

The term "mode" here represents a spatial (not necessarily orthogonal) wavefield component. We use sparse coding to determine the modes and amplitudes present in experimental data (i.e., $\mathbf{V}$). As an illustrative example, a standing wave on a fixed string is represented by a sum of harmonic wave modes with amplitudes corresponding to some excitation. If the mode amplitudes are unknown, we can simulate an impulsive excitation in the string, determine the possible string modes through dictionary learning, and then determine the experimental mode amplitudes with sparse coding. If the string length *and* mode amplitudes are unknown, we can simulate an impulsive excitation in an *infinite* string, determine new possible modes (i.e., a subset of all possible wavelengths), and then determine the experimental mode amplitudes with sparse coding. This demonstrates how we can implicitly incorporate uncertainty (e.g., the string length) into our framework.

Model-Fitting Paradigm: Methods and Result Snapshots

This section describes the model-fitting paradigm methods studied and created throughout this project. These methods use a known analytical model to learn the underlying wave representation.

Sparse Wavenumber Analysis: Sparse Representations For Isotropic Media

Sparse wavenumber analysis determines the global wavenumber (and velocity) characteristics of isotropic materials [62]. For sparse wavenumber analysis, the measurements are usually undersampled (not satisfying the Nyquist-Shannon sampling criteria) in space but densely sampled in time (or data is initially measured in frequency). We model guided Lamb waves $Y(\omega, r)$ between two points (i.e., a transmitter and receiver) of distance r by [62]

$$Y(\omega, r) = \sum_n \sqrt{\frac{1}{k_n(\omega) r}}\, G_n(\omega)\, e^{j k_n(\omega) r} \tag{2}$$

The functions $k_n(\omega)$ and $G_n(\omega)$ represent the frequency-dependent wavenumbers and complex amplitudes for each mode. For an ideal, isotropic plate, $k_n(\omega)$ is the solution to the Rayleigh-Lamb equation [63] and is described by the structure's dispersion curves.

To solve for $k_n(\omega)$ and $G_n(\omega)$, we represent this expression as a matrix multiplication

$$\mathbf{Y} = \mathbf{\Phi V} \tag{3}$$

where $\mathbf{Y}$ is a matrix of data in space and frequency, $\mathbf{V}$ is a dispersion curve matrix, and $\mathbf{\Phi}$ relates the two. The location of elements in $\mathbf{V}$ correspond to the values of $k_n(\omega)$ present in the $\mathbf{Y}$ and the complex amplitudes of $\mathbf{V}$ correspond to the complex amplitudes of $G_n(\omega)$.

An example dispersion curve matrix for an isotropic plate is shown in Figure 3. The figure also illustrates the 50 spatial locations used to extract those dispersion curves. Note that each point has a signal that is densely sampled in time. Figure 4 illustrates our ability to predict full wavefields from this approach information. Note that since reflection information is not included in the analytical model, it does not get predicted. In related work, this fact has been used to create baselines for data without any prior measurements [64–66].

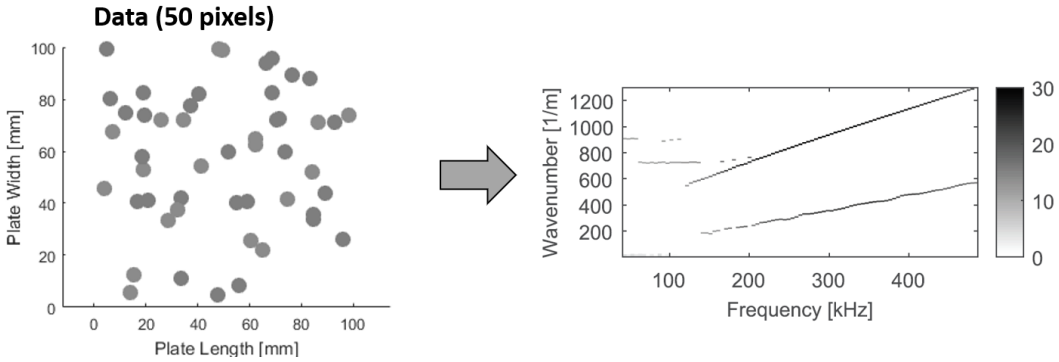

Figure 3: Recovered sparse representation on the right of a set of spatially sparse experimental data on the left. Note that each point in space also have a dense time component. The sparse representation closely resembles the dispersion curves but with amplitudes assigned to each frequency-wavenumber pair.

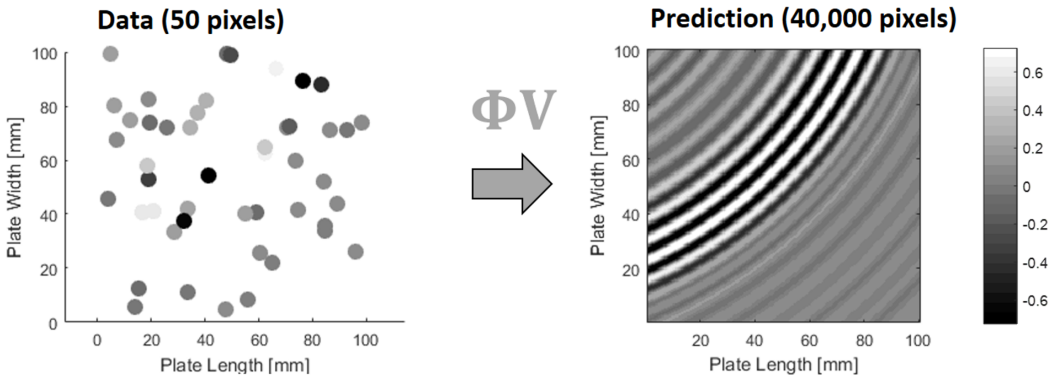

Figure 4: Predicted wavefield on the right from a set of spatially sparse experimental data on the left. Note that each point in space also has a dense time component. The sparse representation closely resembles the dispersion curves but with amplitudes assigned to each frequency-wavenumber pair.

Two-Dimensional Sparse Wavenumber Analysis: Reducing Constraints

Sparse wavenumber analysis can be extended to two dimensions [67, 68], according to

$$Y(\omega, x, y) = \sum_n G_n(\omega)\, e^{j(k_n^{(x)}(\omega)x + k_n^{(y)}(\omega)y)} \tag{4}$$

where x and y are now spatial locations in the two-dimensional space and there are two wavenumbers $k_n^{(x)}(\omega)$ and $k_n^{(y)}(\omega)$ for these corresponding directions. The advantage of this approach is that we do not need to know the source location of the waves and it can address anisotropic wave behavior. The disadvantage is the it requires more data to make an accurate prediction than standard sparse wavenumber analysis. In matrix notation, this setup can be expressed by three matrices

$$\mathbf{Y} = \mathbf{\Phi}_x \mathbf{V} \mathbf{\Phi}_y \tag{5}$$

where $\mathbf{\Phi}_x$ and $\mathbf{\Phi}_y$ translate the two-dimensional dispersion curves in $\mathbf{V}$ in guided wave data in $\mathbf{Y}$. We can also adapt this setup to consider polar coordinates [69] rather than Cartesian coordinates, which simplifies the sparse representation for non-plane wave signals.

Figure 5 illustrates the single-frequency two-dimensional dispersion curves from two-dimensional sparse wavenumber analysis. The left subplot illustrates the results for the Cartesian form and the right subplot illustrates the result for the polar form. Figure 6 illustrates the reconstruction of an anisotropic wavefield (e.g., from a composite material) from approximately 500 sparsely sampled data with two-dimensional sparse wavenumber analysis. Note that standard sparse wavenumber analysis will not work with this data.

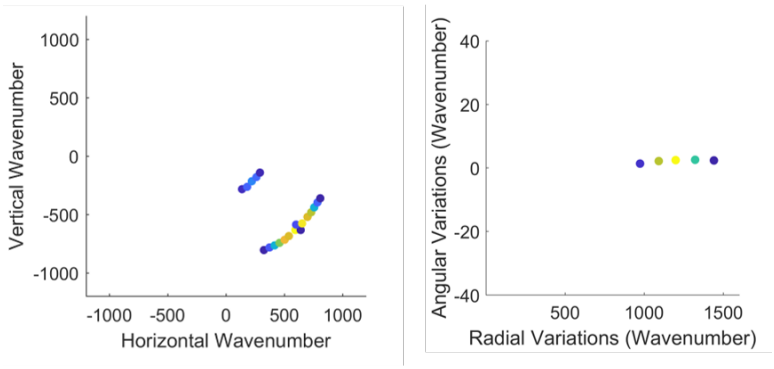

Figure 5: Examples of two-dimensional sparse wavenumber analysis dispersion curves. (Left) illustrates the Cartesian coordinate version and (right) illustrate the Polar coordinate version.

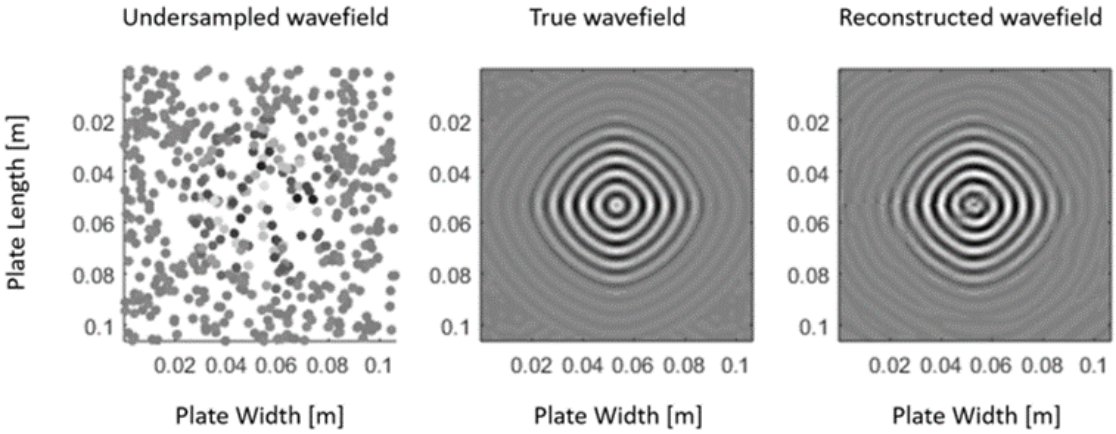

Figure 6: Illustration of prediction of anisotropic guided waves with two-dimensional sparse wavenumber analysis. (left) the measured spatially undersampled data, (center) the true wavefield, (right) the predicted waveform from the two-dimensional dispersion curves learn with the undersampled data.

Anisotropic Sparse Wavenumber Analysis: Sparse Representations for Anisotropic Media

While two-dimensional sparse wavenumber analysis worked with anisotropic media, it required many measurements for good results. One of the issues challenges is that the velocity of propagation varies as a function of direction and we cannot easily estimate the velocity in every possible direction. Therefore, we created an anisotropic sparse wavenumber analysis, which combines aspects of standard sparse wavenumber analysis and two-dimensional sparse wavenumber analysis, to characterize the dependencies between each direction. We created an analytical model for anisotropy [70] defined by

$$Y(\omega, x, y) = \sum_{n} G_n(\omega)\, e^{j((k_n^{(x)}(\omega))^p x + (k_n^{(y)}(\omega))^p y)^{-1/p}} \tag{6}$$

where x represents a horizontal travel distance and y represents a vertical travel distance. The functions $\kappa_n^{(x)}(\omega)$ and $\kappa_n^{(y)}(\omega)$ represent the wavenumbers in the horizontal and vertical directions, respectively. The variable p represents the shape of the wavefront. For example, if $p = 1$, the wavefront is a diamond shape. If $p = 2$, the wavefront is a circle.

The left-most subplot in Figure 7 illustrates $\mathbf{V}$, the experimentally obtained 3D dispersion curves from sparse wavenumber analysis from a glass fiber reinforced polymer plate with 4 aligned unidirectional layers. Each dot in Figure 7 represents a recovered value in frequency(ω)-wavenumber($k^{(x)}$)-wavenumber($k^{(y)}$) space and describes how the waves propagate in the composite. This sparse representation characterizes the entire medium, not just the measured data. As a result, we can use it to predict or extrapolate wave behavior anywhere in the medium. The other two subplots illustrate the predicted wavefield from only 36 time-domain signals across the composite panel.

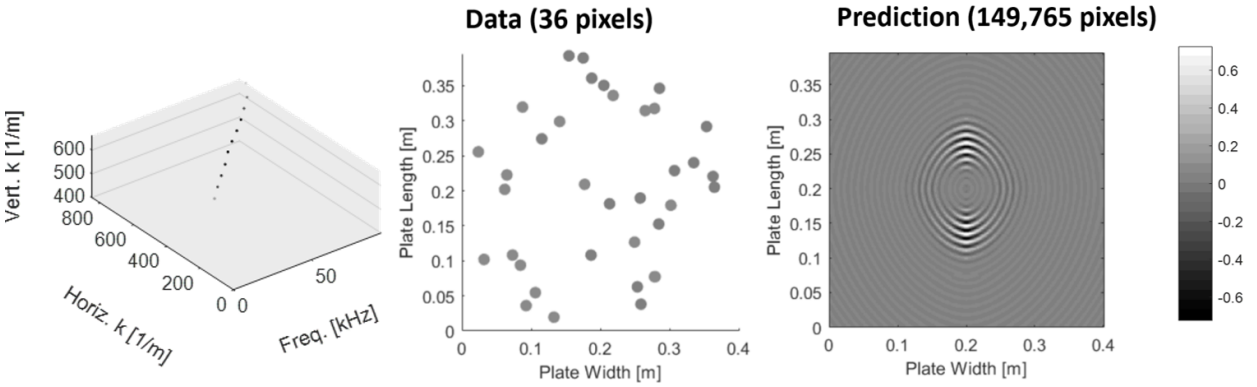

Figure 7: Illustration of anistropic sparse wavenumber analysis. (left) Anisotropic dispersion curve. (center) Sparsely sampled measurement locations in space. (right) Predicted wavefield reconstructed from the anisotropic dispersion curve and sparse sampled data.

Temporal Sparse Wavenumber Analysis: Sparse Representations for Undersampling Time

Temporal sparse wavenumber analysis [67] determines the global frequency (and velocity) characteristics of isotropic materials but sampled sparsely in time rather than space. Hence we can reduce the amount of data needed by sampling measurements slower. For temporal sparse wavenumber analysis, the measurements are usually undersampled (not satisfying the Nyquist-Shannon sampling criteria) in time but densely sampled in space. The setup for temporal sparse wavenumber analysis is similar to the setup for regular sparse wavenumber analysis, but to solve the inverse problem (identify $k_n(\omega)$ and $G_n(\omega)$), we represent this expression as a different matrix multiplication

$$\mathbf{Y} = \mathbf{V}\mathbf{\Psi}^H \tag{7}$$

where $\mathbf{Y}$ is a matrix of data of wavenumber and time, $\mathbf{V}$ is a dispersion curve matrix, and $\mathbf{\Psi}$ relates the two. The location of elements in $\mathbf{V}$ correspond to the values of $k_n(\omega)$ present in the $\mathbf{Y}$ and the complex amplitudes of $\mathbf{V}$ correspond to the complex amplitudes of $G_n(\omega)$.

An example prediction from temporal sparse wavenumber analysis is shown in Figure 8. The left-most subplot shows the undersampled time-domain signal with only 15 samples. The reconstructed and true signals have 2000 samples. This demonstrates that we can learn and predict wave behavior with very little input data.

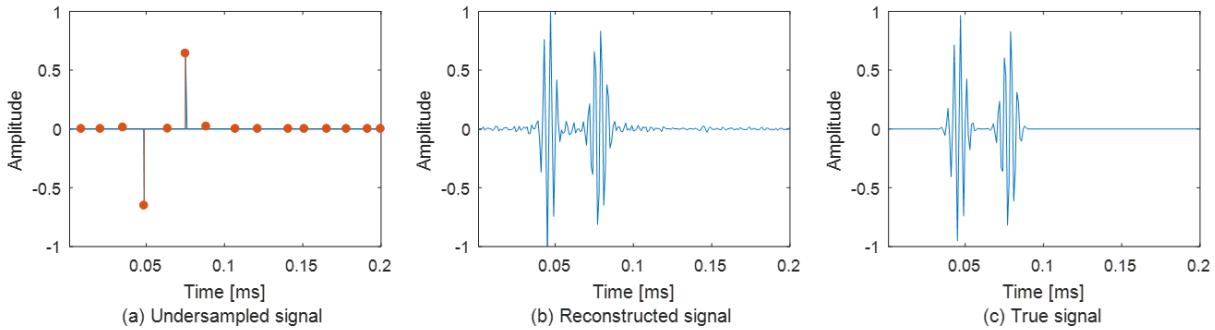

Figure 8: Illustration of temporal sparse wavenumber analysis results. (left) The temporally undersampled data. (center) The predicted temporal signal based on the dispersion curves learned by the undersampled data. (right) The true densely sampled signal.

Spatio-Temporal Sparse Wavenumber Analysis: Undersampling in Time and Space

Spatio-temporal sparse wavenumber analysis [71] determines the global frequency-wavenumber characteristics of isotropic materials. For spatio-temporal sparse wavenumber analysis, the measurements are usually undersampled (not satisfying the Nyquist-Shannon sampling criteria) in both time and space. To solve for $k_n(\omega)$ and $G_n(\omega)$, we represent this expression as a matrix multiplication

$$\mathbf{Y} = \mathbf{\Phi}\mathbf{V}\mathbf{\Psi}^H \tag{8}$$

where $\mathbf{Y}$ is a matrix of data of space and time and $\mathbf{V}$ is a dispersion curve matrix. The matrix $\mathbf{\Phi}$ relates space to wavenumber. The matrix $\mathbf{\Psi}$ relates time to frequency. An example prediction is shown in Figure 9. The left-most subplot shows the undersampled spatial information, which changes with each point in time (i.e., the data is not dense in time). We predict the signals with 40% less data than required by the Nyquist-Shannon sampling criteria.

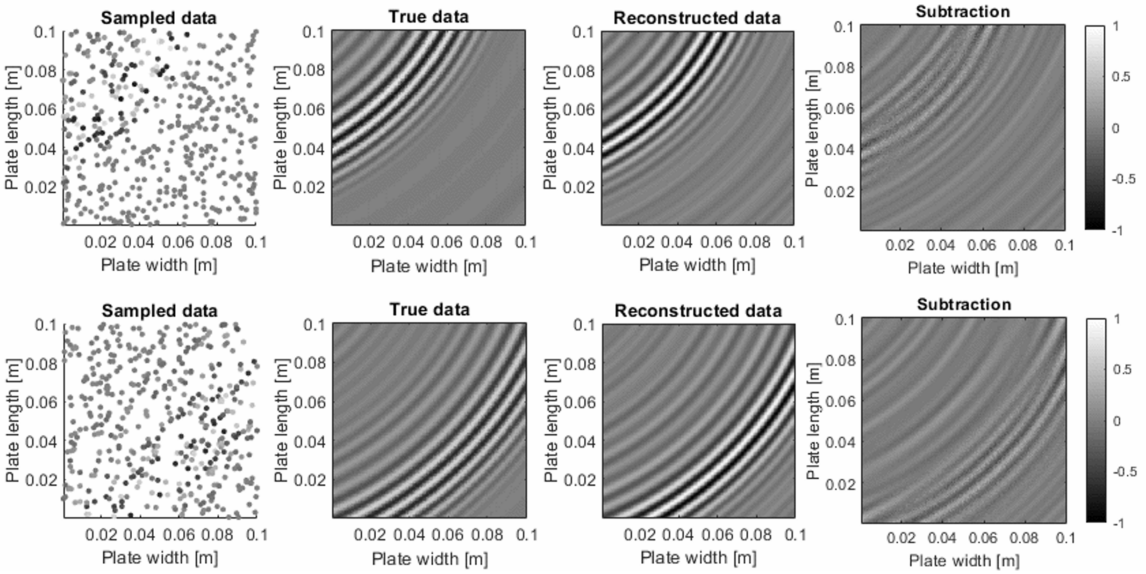

Figure 9: Illustration of spatio-temporal sparse wavenumber analysis. From left to right, the columns show two time snapshots of undersampled wavefields, the experimentally measured wavefields, the predicted wavefields from the undersampled data dispersion curves, and the subtraction between the true and predicted data.

Transfer Learning Paradigm: Methods and Result Snapshots

Dictionary Learning (Experiment-to-Experiment)

Sparse coding requires a known dictionary of modes $\mathbf{\Phi}$. For complex structures, manually deriving $\mathbf{\Phi}$ becomes very difficult very quickly. Therefore, we need a method to numerically determine $\mathbf{\Phi}$. That is, we need a method that will find an appropriate $\mathbf{\Phi}$ matrix of modes given a numerical simulation. Algorithms that can determine $\mathbf{\Phi}$ are known as dictionary learning algorithms [14, 72–74]. Dictionary learning methods such as K-SVD [14, 72, 73], MOD [75], and Sparsenet [76] determine the dictionary for which there is a sparse representation $\mathbf{V}$. Although less well understood than the sparse coding methods, theoretical and empirical results show that dictionary learning achieves accurate results as long as there exists some matrix $\mathbf{V}$ that is sparse [77].

We can train our dictionary from either surrogate experimental data (measured data originating from a similar structural geometry but different wave behavior) or similar simulation data. Figure 10 illustrates the prediction and baseline subtraction achieved using an experimental surrogate [78]. This considers data from a small 10cm by 10cm plate with abundant reflections. We refer to this as an experiment-to-experiment approach. The top row in the figure illustrates the subtraction of a wavefield from an aluminum plate with a mass, emulating a flaw, located on it (i.e., the white dotted circle) and the surrogate steel structure. We observe that the subtraction does not improve our ability to detect the reflections from the mass. The bottom row illustrates the same process, but a dictionary $\mathbf{\Phi}$ was trained from the surrogate and the sparse representation $\mathbf{V}$ was learned from the test structure. This enabled a better subtraction, where the reflection from the mass is observable.

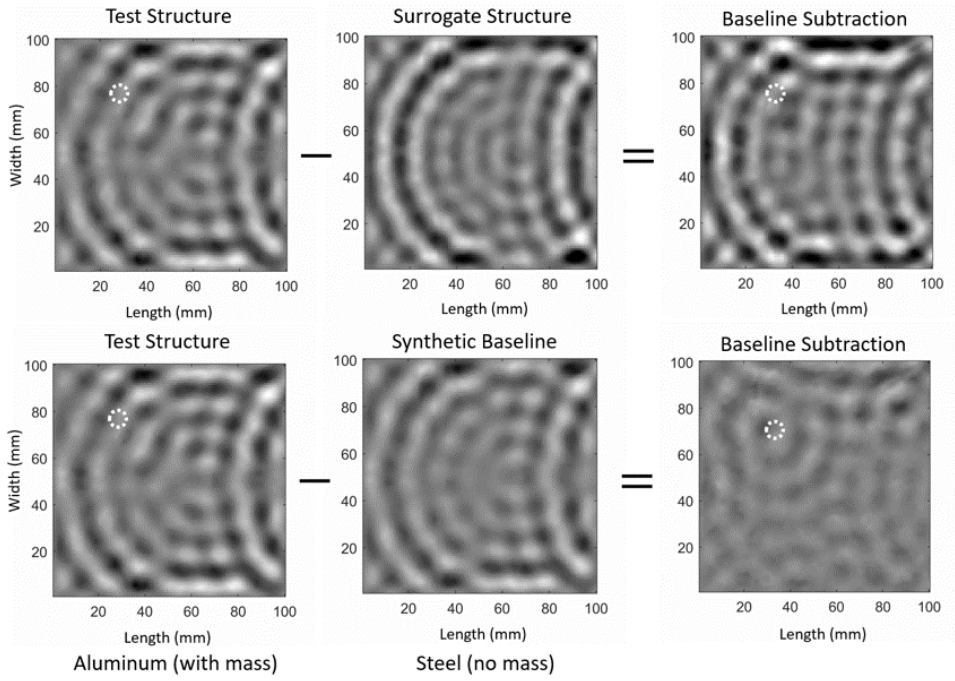

Figure 10: Illustration using dictionary learning to learn from the underlying representation of a wavefield experimental data and then adapt it to different experimental data. The top row illustrates the subtraction between two similar datasets without the dictionary learning adaptation. The bottom row illustrates the subtraction between the same datasets with the dictionary learning adaptation.

Dictionary Learning (Simulation-to-Experiment)

Figure 11 illustrates the prediction and baseline subtraction achieved using a simulated surrogate. This considers data from a 0.5m by 0.5m non-square aluminum panel (creating unusual boundary reflections) and multiple (which create additional reflections) [79]. We refer to this as a simulation-to-experiment (or sim-to-real) approach. The figure illustrates an experiment with a flaw and simulation data of the same geometry but very different wave behavior. We train $\mathbf{\Phi}$ with the simulation data and then train $\mathbf{V}$ with that dictionary and the experimental data. The reconstructed signal contains the geometric information of the simulation but the wave behavior of the experiment. This enables us to subtract away the incident wavefront and retain reflections from the defect.

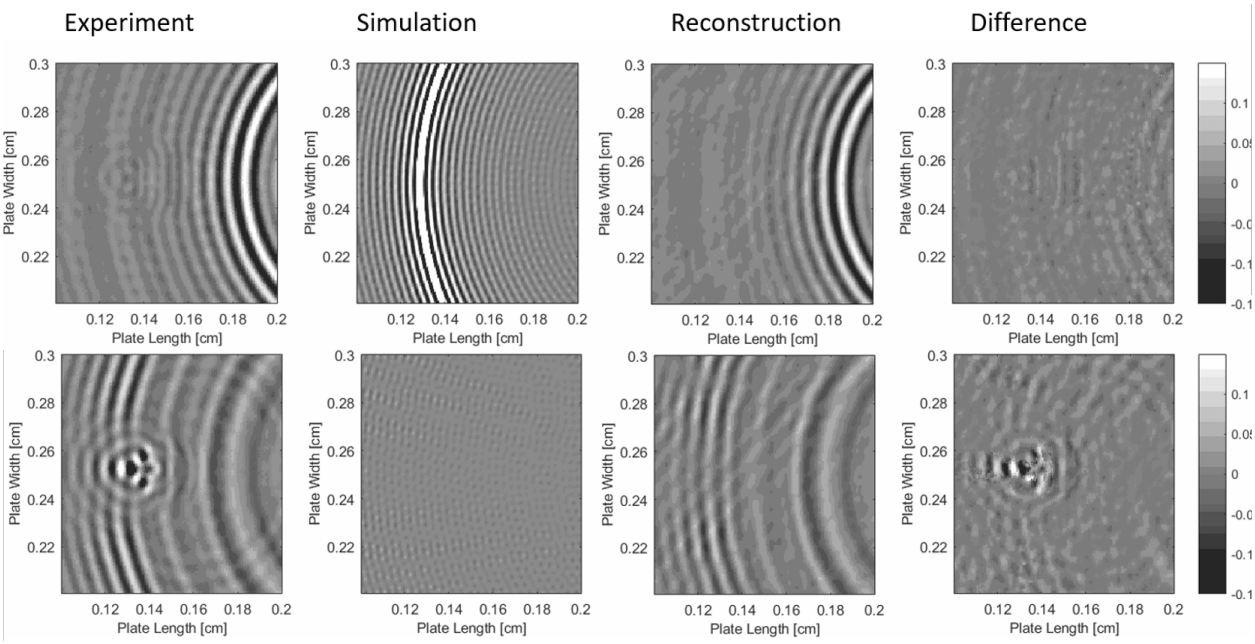

Figure 11: Illustration using dictionary learning to learn from the underlying representation of a wavefield simulation data and then adapt it to visually different experimental data. From left to right, the subplot columns show two different time snapshots of the original experimental data with a defect, the simulation used to train the dictionary, the predicted wavefield from the dictionary and the experimental data, and the difference between the experimental data and the prediction. This difference highlights the reflection from the defect without any explicit baseline.

Transfer Learning with Sparse Autoencoders

In deep learning theory, a sparse autoencoder neural network has a close relationship with dictionary learning algorithms. As a result, the sparse autoencoder can be used in much the same manner. The difference is that the sparse autoencoder can exploit nonlinearity in the data whereas dictionary learning assumes a purely linear machine learning model.

Figure 12 illustrates a preliminary result from a sparse autoencoder [80]. This example trains the dictionary (the weights of the neural network) using simulated surrogate data and reconstructs wavefield data with different wave behavior. The second subplot illustrates one set of weights from the neural network to show that the neural network learns mode-like components from the surrogate

simulation data. The results show that the autoencoder can also predict wave behavior. However, we generally found dictionary learning to outperform the sparse autoencoder. We hypothesis that this is because the neural network architecture cannot be used natively with complex numbers (necessary since we work in the Fourier domain) whereas dictionary learning does. We believe the workarounds needed to make the autoencoder work reduce its overall performance.

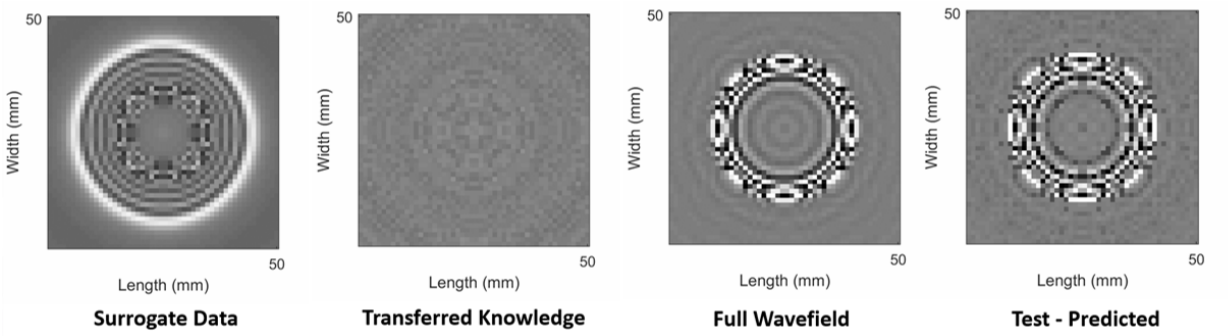

Figure 12: Illustration using a sparse autoencoder learning to learn from the underlying representation of a wavefield simulation data and then adapt it to visually different simulation data. From left to right, the subplots show the simulation used to train the dictionary, an example weight generated in the neural network, the different simulated data, and the predicted wavefield from the trained dictionary and the different simulated data.

Wave-Informed Dictionary Learning

We have also had preliminary efforts into creating a wave-informed, or more generally a physics-informed, dictionary learning algorithm. The advantage of this approach is that the dictionary elements are required to satisfy the wave equation. In addition, we can extract our wave equation parameters (namely, the wavenumbers of the learned dictionary element) directly from the algorithm. This information is not extracted from the traditional dictionary learning algorithm. As a result, this algorithm is more robust and more interpretable than the traditional dictionary learning algorithm. Papers on this topic are still being prepared for eventual publication.

Conclusions and Future Work

This work establishes the fundamental theory for integrating analytical and numerical models with experimental data. Future work aims to build on the preliminary wave-informed learning efforts originated in this proposal. More generally, the Smart Diagnostics, Acoustics, and Time-series Analysis (SmartDATA) Lab aims to use this technology to integrate physical properties and laws of nature into state-of-the-art data analysis, machine learning, and signal processing techniques. This will require us to address three critical challenges in analyzing and understanding complex, physical systems and materials: (1) collecting sufficient amounts of data is often impossible for practical and financial reasons, (2) capturing the data diversity for informed decision-making can be impossible due to insufficient laboratory conditions or lack of observations (i.e., rare events), and (3) data-driven analytics are not explainable like with physics-based techniques. Future work will focus on addressing these three challenges.

References Cited

[1] C. A. C. Leckey, M. D. Rogge, and F. Raymond Parker, "Guided waves in anisotropic and quasi-isotropic aerospace composites: three-dimensional simulation and experiment," *Ultrasonics*, vol. 54, no. 1, pp. 385–394, Jan. 2014.

[2] A. A. Nasedkina, A. Alexiev, and J. Malachowski, "Numerical simulation of ultrasonic torsional guided wave propagation for pipes with defects," in *Advanced Materials*, ser. Springer Proceedings in Physics, I. A. Parinov, S.-H. Chang, and V. Y. Topolov, Eds. Springer International Publishing, 2016, pp. 475–488.

[3] Y. Shen and V. Giurgiutiu, "WaveFormRevealer: an analytical framework and predictive tool for the simulation of multi-modal guided wave propagation and interaction with damage," *Structural Health Monitoring*, 2014.

[4] J. B. Harley and J. M. F. Moura, "Scale transform signal processing for optimal ultrasonic temperature compensation," *IEEE Trans. Ultrason. Ferroelectr. Freq. Control*, vol. 59, no. 10, pp. 2226–2236, Oct. 2012.

[5] F. Chen and P. D. Wilcox, "The effect of load on guided wave propagation," *Ultrasonics*, vol. 47, no. 1-4, pp. 111–122, Dec. 2007.

[6] V. A. Attarian, F. B. Cegla, and P. Cawley, "Long-term stability of guided wave structural health monitoring using distributed adhesively bonded piezoelectric transducers," *Structural Health Monitoring*, vol. 13, no. 3, pp. 265–280, May 2014.

[7] D. F. Gingras, "Inversion for geometric and geoacoustic parameters in shallow water: Experimental results," *J. Acoust. Soc. Am.*, vol. 97, no. 6, p. 3589, 1995.

[8] P. Santos, J. Joao, O. C. Rodriguez, P. Felisberto, and S. M. Jesus, "Geometric and seabed parameter estimation using a vector sensor array - experimental results from makai experiment 2005," in *Proc. of OCEANS*. Santander: IEEE, Jun. 2011, pp. 1–10.

[9] J. S. Hall and J. E. Michaels, "Model-based parameter estimation for characterizing wave propagation in a homogeneous medium," *Inverse Probl.*, vol. 27, no. 3, p. 035002, Mar. 2011.

[10] M. Gresil and V. Giurgiutiu, "Prediction of attenuated guided waves propagation in carbon fiber composites using rayleigh damping model," *J. Intell. Mater. Syst. Struct.*, vol. 26, no. 16, pp. 2151–2169, Nov. 2015.

[11] V. Giurgiutiu, M. Gresil, B. Lin, A. Cuc, Y. Shen, and C. Roman, "Predictive modeling of piezoelectric wafer active sensors interaction with high-frequency structural waves and vibration," *Acta Mech.*, vol. 223, no. 8, pp. 1681–1691, Mar. 2012.

[12] E. J. Candès and M. B. Wakin, "An introduction to compressive sampling," *IEEE Signal Process. Mag.*, vol. 25, no. 2, pp. 21–30, Mar. 2008.

[13] D. L. Donoho, M. Elad, and V. N. Temlyakov, "Stable recovery of sparse overcomplete representations in the presence of noise," *IEEE Trans. Inf. Theory*, vol. 52, no. 1, pp. 6–18, Jan. 2006.

[14] M. Aharon, M. Elad, and A. Bruckstein, "K-SVD: An algorithm for designing overcomplete dictionaries for sparse representation," *IEEE Trans. Signal Process.*, vol. 54, no. 11, pp. 4311–4322, Nov. 2006.

[15] P. Cawley, "Practical long range guided wave inspection – managing complexity," in *Proc. of the Review of Progress in Quantitative Nondestructive Evaluation*, vol. 22, Jul. 2003, pp. 22–40.

[16] ——, "Practical guided wave inspection and applications to structural health monitoring," in *Proc. of the Australasian Congress on Applied Mechanics*, Brisbane, Dec. 2007, p. 10.

[17] ——, "Structural health monitoring: Closing the gap between research and industrial deployment," *Structural Health Monitoring*, vol. 17, no. 5, pp. 1225–1244, Sep. 2018.

[18] J. Davies and P. Cawley, "The application of synthetic focusing for imaging crack-like defects in pipelines using guided waves," *IEEE Trans. Ultrason. Ferroelectr. Freq. Control*, vol. 56, no. 4, pp. 759–771, Apr. 2009.

[19] C. Liu, J. Harley, N. O'Donoughue, Y. Ying, M. H. Altschul, M. Bergés, J. H. Garrett, D. W. Greve, J. M. F. Moura, I. J. Oppenheim, and L. Soibelman, "Robust change detection in highly dynamic guided wave signals with singular value decomposition," in *2012 IEEE International Ultrasonics Symposium*. Dresden: IEEE, Oct. 2012, pp. 483–486.

[20] Y. Ying, L. Soibelman, J. Harley, N. O'Donoughue, J. H. Garrett, Y. Jin, J. M. F. Moura, and I. J. Oppenheim, "A data mining framework for pipeline monitoring using time reversal," in *Proc. of SIAM Conference on Data Mining*. Columbus, Ohio: SIAM, Apr. 2010.

[21] Y. Ying, J. H. Garrett, Jr., J. Harley, I. J. Oppenheim, J. Shi, and L. Soibelman, "Damage detection in pipes under changing environmental conditions using embedded piezoelectric transducers and pattern recognition techniques," *J. Pipeline Syst. Eng. Pract.*, vol. 4, no. 1, pp. 17–23, Feb. 2013.

[22] P. Rizzo, I. Bartoli, A. Marzani, and F. L. di Scalea, "Defect classification in pipes by neural networks using multiple guided ultrasonic wave features extracted after wavelet processing," *J. Pressure Vessel Technol.*, vol. 127, no. 3, pp. 294–303, Aug. 2005.

[23] J. Li and J. Rose, "Angular-Profile tuning of guided waves in hollow cylinders using a circumferential phased array," *IEEE Trans. Ultrason. Ferroelectr. Freq. Control*, vol. 49, no. 12, pp. 1720–1729, Dec. 2002.

[24] S. Chen, F. Cerda, J. Guo, J. B. Harley, Q. Shi, P. Rizzo, J. Bielak, J. H. Garrett, and J. Kovačević, "Multiresolution classification with semi-supervised learning for indirect bridge structural health monitoring," in *2013 IEEE International Conference on Acoustics, Speech and Signal Processing*. Vancouver, BC: IEEE, May 2013, pp. 3412–3416.

[25] K. M. Holford, A. W. Davies, R. Pullin, and D. C. Carter, "Damage location in steel bridges by acoustic emission," *J. Intell. Mater. Syst. Struct.*, vol. 12, no. 8, pp. 567–576, Aug. 2001.

[26] K. P. Chong, N. J. Carino, and G. Washer, "Health monitoring of civil infrastructures," *Smart Mater. Struct.*, vol. 12, no. 3, pp. 483–493, Jun. 2003.

[27] A. Baltazar, C. D. Hernandez-Salazar, and B. Manzanares-Martinez, "Study of wave propagation in a multiwire cable to determine structural damage," *NDT and E Int.*, vol. 43, no. 8, pp. 726–732, 2010.

[28] P. Rizzo, "Wave propagation in Multi-Wire strands by Wavelet-Based laser ultrasound," *Exp. Mech.*, vol. 44, no. 4, pp. 407–415, 2004.

[29] P. Rizzo and F. Lanza di Scalea, "Acoustic emission monitoring of carbon-fiber-reinforced-polymer bridge stay cables in large-scale testing," *Exp. Mech.*, vol. 41, no. 3, pp. 282–290, Sep. 2001.

[30] J.-B. Ihn and F.-K. Chang, "Pitch-catch active sensing methods in structural health monitoring for aircraft structures," *Structural Health Monitoring*, vol. 7, no. 1, pp. 5–19, Mar. 2008.

[31] K. Worden, G. Manson, and D. Allman, "Experimental validation of a structural health monitoring methodology: Part i. novelty detection on a laboratory structure," *J. Sound Vib.*, vol. 259, no. 2, pp. 323–343, Jan. 2003.

[32] W. J. Staszewski, S. Mahzan, and R. Traynor, "Health monitoring of aerospace composite structures – active and passive approach," *Compos. Sci. Technol.*, vol. 69, no. 11-12, pp. 1678–1685, Sep. 2009.

[33] L. Qiu, S. Yuan, X. Zhang, and Y. Wang, "A time reversal focusing based impact imaging method and its evaluation on complex composite structures," *Smart Mater. Struct.*, vol. 20, no. 10, p. 105014, Oct. 2011.

[34] S. Salamone, I. Bartoli, F. Lanza Di Scalea, and S. Coccia, "Guided-wave health monitoring of aircraft composite panels under changing temperature," *J. Intell. Mater. Syst. Struct.*, vol. 20, no. 9, pp. 1079–1090, Jun. 2009.

[35] T. Clarke, F. Simonetti, and P. Cawley, "Guided wave health monitoring of complex structures by sparse array systems: Influence of temperature changes on performance," *J. Sound Vib.*, vol. 329, no. 12, pp. 2306–2322, Jun. 2010.

[36] T. Clarke and P. Cawley, "Enhancing the defect localization capability of a guided wave SHM system applied to a complex structure," *Struct. Health Monit.*, vol. 10, no. 3, pp. 247–259, Jun. 2010.

[37] J. B. Harley and J. M. F. Moura, "Sparse recovery of the multimodal and dispersive characteristics of lamb waves," *J. Acoust. Soc. Am.*, vol. 133, no. 5, pp. 2732–2745, May 2013.

[38] J. Hall and J. E. Michaels, "Minimum variance ultrasonic imaging applied to an in situ sparse guided wave array," *IEEE Trans. Ultrason. Ferroelectr. Freq. Control*, vol. 57, no. 10, pp. 2311–2323, Oct. 2010.

[39] L. Yu and Z. Tian, "Guided wave phased array beamforming and imaging in composite plates," *Ultrasonics*, vol. 68, pp. 43–53, Feb. 2016.

[40] G. C. McLaskey, S. D. Glaser, and C. U. Grosse, "Beamforming array techniques for acoustic emission monitoring of large concrete structures," *J. Sound Vib.*, vol. 329, no. 12, pp. 2384–2394, Jun. 2010.

[41] Y. Jin and J. M. F. Moura, "Time-Reversal detection using antenna arrays," *IEEE Trans. Signal Process.*, vol. 57, no. 4, pp. 1396–1414, Apr. 2009.

[42] P. Blomgren, G. Papanicolaou, and H. Zhao, "Super-resolution in time-reversal acoustics," *J. Acoust. Soc. Am.*, vol. 111, no. 1 Pt 1, pp. 230–248, Jan. 2002.

[43] B. Park, H. Sohn, S. E. Olson, M. P. DeSimio, K. S. Brown, and M. M. Derriso, "Impact localization in complex structures using laser-based time reversal," *Structural Health Monitoring*, vol. 11, no. 5, pp. 577–588, Sep. 2012.

[44] J. E. Michaels, "Detection, localization and characterization of damage in plates with an in situ array of spatially distributed ultrasonic sensors," *Smart Mater. Struct.*, vol. 17, no. 3, p. 035035, May 2008.

[45] J. B. Harley, N. Thavornpitak, and J. M. F. Moura, "Delay-and-sum technique for localization of active sources in cylindrical objects," in *Proc. of the Review of Progress in Nondestructive Evaluation*, ser. AIP Conference Proceedings, vol. 1511. AIP, 2013, pp. 294–301.

[46] J. S. Hall, P. McKeon, L. Satyanarayan, J. E. Michaels, N. F. Declercq, and Y. H. Berthelot, "Minimum variance guided wave imaging in a quasi-isotropic composite plate," *Smart Mater. Struct.*, vol. 20, no. 2, p. 025013, 2011.

[47] N. Testoni, L. De Marchi, and A. Marzani, "Detection and characterization of delaminations in composite plates via air-coupled probes and warped-domain filtering," *Compos. Struct.*, vol. 153, pp. 773–781, Oct. 2016.

[48] J. E. Michaels, D. E. Chimenti, and L. J. Bond, "Ultrasonic wavefield imaging: Research tool or emerging NDE method?" *AIP Conf. Proc.*, vol. 1806, no. 1, p. 020001, Feb. 2017.

[49] E. B. Flynn, S. Y. Chong, G. J. Jarmer, and J. R. Lee, "Structural imaging through local wavenumber estimation of guided waves," *NDT and E Int.*, vol. 59, pp. 1–10, 2013.

[50] Z. Tian, L. Yu, and C. Leckey, "Rapid guided wave delamination detection and quantification in composites using global-local sensing," *Smart Mater. Struct.*, vol. 25, no. 8, p. 085042, Jul. 2016.

[51] O. Mesnil, C. A. C. Leckey, and M. Ruzzene, "Instantaneous and local wavenumber estimations for damage quantification in composites," *Structural Health Monitoring*, vol. 14, no. 3, pp. 193–204, May 2015.

[52] C. Leckey, E. Frankforter, M. Horne, and W. Schneck, "Modeling of guided waves for aerospace applications," in *Health Monitoring of Structural and Biological Systems XV*, vol. 11593. International Society for Optics and Photonics, Mar. 2021, p. 1159305.

[53] M. Geradin and D. J. Rixen, "Solution methods for the eigenvalue problem," in *Mechanical Vibrations: Theory and Application to Structural Dynamics*, 3rd ed. Chichester: John Wiley & Sons, 2015, pp. 415–510.

[54] E. Moulin, J. Assaad, C. Delebarre, and D. Balageas, "A coupled finite-element–normal modes expansion method to model lamb waves generated with integrated transducers in composite plates," *J. Acoust. Soc. Am.*, vol. 105, no. 1, p. 1241, 1999.

[55] D. L. Donoho, "Compressed sensing," *IEEE Trans. Inf. Theory*, vol. 52, no. 4, pp. 1289–1306, Apr. 2006.

[56] M. A. Davenport, M. F. Duarte, Y. C. Eldar, and G. Kutyniok, "Introduction to compressed sensing," in *Compressed Sensing: Theory and Applications*, Y. C. Eldar and G. Kutyniok, Eds. Cambridge: Cambridge University Press, 2012, pp. 1–68.

[57] M. F. Duarte, M. A. Davenport, D. Takhar, J. N. Laska, K. F. Kelly, and R. G. Baraniuk, "Single-pixel imaging via compressive sampling," *IEEE Signal Process. Mag.*, vol. 25, no. 2, pp. 83–91, Mar. 2008.

[58] O. G. Guleryuz, "Nonlinear approximation based image recovery using adaptive sparse reconstructions and iterated denoising-part i: theory," *IEEE Trans. Image Process.*, vol. 15, no. 3, pp. 539–554, Mar. 2006.

[59] J. V. Shi, A. C. Sankaranarayanan, C. Studer, and R. G. Baraniuk, "Video compressive sensing for dynamic MRI," *BMC Neurosci.*, vol. 13, no. Suppl 1, p. P183, 2012.

[60] M. Lustig, D. L. Donoho, J. M. Santos, and J. M. Pauly, "Compressed sensing MRI," *IEEE Signal Process. Mag.*, vol. 25, no. 2, pp. 72–82, Mar. 2008.

[61] F. Herrmann, M. Friedlander, and O. Yilmaz, "Fighting the curse of dimensionality: compressive sensing in exploration seismology," *IEEE Signal Process. Mag.*, vol. 29, no. 3, pp. 88–100, May 2012.

[62] J. B. Harley and J. M. F. Moura, "Dispersion curve recovery with orthogonal matching pursuit," *J. Acoust. Soc. Am.*, vol. 137, no. 1, pp. EL1–7, Jan. 2015.

[63] K. Graff, "Waves and vibrations in strings," in *Wave Motion in Elastic Solids*, 1st ed. New York: Dover Publications, 1975, pp. 9–74.

[64] J. B. Harley and J. M. F. Moura, "Data-driven matched field processing for lamb wave structural health monitoring," *J. Acoust. Soc. Am.*, vol. 135, no. 3, pp. 1231–1244, Mar. 2014.

[65] ——, "Data-driven and calibration-free lamb wave source localization with sparse sensor arrays," *IEEE Trans. Ultrason. Ferroelectr. Freq. Control*, vol. 62, no. 8, pp. 1516–1529, Aug. 2015.

[66] J. B. Harley, "Predictive guided wave models through sparse modal representations," *Proc. IEEE*, vol. 104, no. 8, pp. 1604–1619, Aug. 2016.

[67] S. Sabeti and J. B. Harley, "Guided wave retrieval from temporally undersampled data," in *2017 IEEE International Ultrasonics Symposium (IUS)*, Sep. 2017, pp. 1–4.

[68] ——, "Two-dimensional sparse wavenumber recovery for guided wavefields," in *Proc. of the Review of Quantitative Nondestructive Evaluation*, vol. 1949. American Institute of Physics, Apr. 2018, p. 230003.

[69] ——, "Polar sparse wavenumber analysis for guided wave reconstruction," in *Proc. of the Review of Quantitative Nondestructive Evaluation*, vol. 2102. American Institute of Physics, May 2019, p. 050012.

[70] S. Sabeti, C. A. C. Leckey, L. De Marchi, and J. B. Harley, "Sparse wavenumber recovery and prediction of anisotropic guided waves in composites: A comparative study," *IEEE Trans. Ultrason. Ferroelectr. Freq. Control*, May 2019.

[71] S. Sabeti and J. B. Harley, "Spatio-temporal undersampling: Recovering ultrasonic guided wavefields from incomplete data with compressive sensing," *Mech. Syst. Signal Process.*, vol. 140, p. 106694, Jun. 2020.

[72] Z. Jiang, Z. Lin, and L. S. Davis, "Learning a discriminative dictionary for sparse coding via label consistent K-SVD," in *Proc. of the IEEE Conference on Computer Vision and Pattern Recognition*, Jun. 2011, pp. 1697–1704.

[73] R. Rubinstein, T. Peleg, and M. Elad, "Analysis K-SVD: A Dictionary-Learning algorithm for the analysis sparse model," *Signal Processing, IEEE Transactions on*, vol. 61, no. 3, pp. 661–677, Feb. 2013.

[74] I. Tosic and P. Frossard, "Dictionary learning," *Signal Processing Magazine, IEEE*, vol. 28, no. 2, pp. 27–38, Mar. 2011.

[75] K. Engan, S. O. Aase, and J. H. Husoy, "Frame based signal compression using method of optimal directions (MOD)," in *Circuits and Systems, 1999. ISCAS '99. Proceedings of the 1999 IEEE International Symposium on*, vol. 4. ieeexplore.ieee.org, Jul. 1999, pp. 1–4 vol.4.

[76] B. Mailhé and M. D. Plumbley, "Dictionary learning with large step gradient descent for sparse representations," in *Latent Variable Analysis and Signal Separation*, ser. Lecture Notes in Computer Science. Springer Berlin Heidelberg, 2012, pp. 231–238.

[77] Q. Geng and J. Wright, "On the local correctness of $\ell 1$-minimization for dictionary learning," in *Information Theory (ISIT), 2014 IEEE International Symposium on*. ieeexplore.ieee.org, 2014, pp. 3180–3184.

[78] K. S. Alguri, J. Melville, and J. B. Harley, "Baseline-free guided wave damage detection with surrogate data and dictionary learning," *J. Acoust. Soc. Am.*, vol. 143, no. 6, p. 3807, Jun. 2018.

[79] K. S. Alguri, C. C. Chia, and J. B. Harley, "Sim-to-Real: Employing ultrasonic guided wave digital surrogates and transfer learning for damage visualization," *Ultrasonics*, vol. 111, p. 106338, Mar. 2021.

[80] K. S. Alguri and J. B. Harley, "Transfer learning of ultrasonic guided waves using autoencoders: A preliminary study," in *Proc. of the Review of Quantitative Nondestructive Evaluation*, vol. 2102. American Institute of Physics, May 2019, p. 050013.